Preparation of Enantiomerically Pure Chelate Ligands L_2 = $XCH_2CH(OH)CH_2Y$ from Epichlorohydrin – Conformation of Their $L_2Rh(COD)^+$ Derivatives and Enantioselective Hydrogenation by $L_2Rh(COD)^+$

Jörg Karas,[a] Gottfried Huttner,*[a] Katja Heinze,[a] Peter Rutsch,[a] and Laszlo Zsolnai[a]

In memoriam of Laszlo Zsolnai

Keywords: Epichlorohydrin / Chiral diphos ligands / Diphos rhodium complexes / Conformation analysis / Chelates / Asymmetric synthesis

Enantiomerically pure chelate ligands L_2 = $XCH_2CH(OH)CH_2Y$ (**1**) are obtained from epichlorohydrin in a two-step synthesis. X and Y may be different types of R_2P donor groups, NR_2 or SR donors. The OH function of **1** may be transformed into an ether function under specialized conditions. Ligands **1** react with $[Rh(COD)Cl]_2$ in the presence of KPF_6 to give the coordination compounds **2**, $[L_2Rh(COD)]^+PF_6^-$, as orange, microcrystalline salts. The structures adopted by compounds **2** in the solid state have been analysed by X-ray crystallography in selected cases, and it has been found that the six-membered chelate cycles adopt twist as well as chair conformations depending on the nature of X and Y. In solution, compounds **2** generally show dynamic behaviour, which is in part due to the conformational flexibility of the six-membered cycles. In cases where one of the PR_2 donor groups contains *ortho*-substituted phenyl substituents, rotational isomerism of these groups is an additional dynamic process. For some of these compounds, the nature of the dynamic behaviour has been analysed by variable-temperature NMR experiments. Compounds **2** are found to be precatalysts in the hydrogenation of (*Z*)-2-acetamidocinnamic acid. The rate of conversion is strongly influenced by the steric bulk of the substituents, with smaller substituents leading to higher rates. Enantiomeric discrimination is high only for those ligands that contain *ortho*-substituted aryl groups at their PR_2 donors. The maximum enantiomeric excess observed was 85% for X = PPh_2, Y = $P(2\text{-MeOPh})_2$.

Introduction

Enantioselective hydrogenation mediated by chiral bis(phosphane)rhodium templates is a well-established process.[1,2] Even though the major steps of the relevant catalytic cycles are well known,[3] there is still no means of predicting which properties of the ligands will induce a high enantioselectivity. It has been found that chelate diphosphane ligands are generally a good choice.[4,5] From the data available to date, it appears that five-membered and seven-membered cycles are superior to six-membered chelate rings in this respect.[2] In almost all of the relevant chelate ligands, chirality is embedded in the backbone, and this again appears to be a good principle, in particular because building blocks for the chiral backbones are often readily available from the chiral pool.[5] Despite the existence of a large amount of relevant literature,[6] there is no straightforward way of predicting the efficiency of a specific ligand.

As far as six-membered chelate cycles are concerned, their generally low efficiency has been attributed to the particular conformational flexibility of these cycles, which allows both chair and twist conformations, although only the twist conformations induce strong enantiomeric discrimination.[7] In solid-state structures, both conformations have been observed, even with the same chelate ligand. Thus, (2*S*,4*S*)-2,4-bis(diphenylphosphanyl)pentane $Ph_2PCH(CH_3)CH_2CH(CH_3)PPh_2$ (skewphos) forms a chelate chair with norbornadiene (NBD) as a coligand in the catalyst precursor skewphosRh(NBD)$^+$, while it is found in the twist conformation with cyclooctadiene (COD) as a coligand in skewphosRh(COD)$^+$.[8,9] Even though the chair conformation is thus available to this specific chelate cycle, it holds the record for enantioselectivity (*ee* > 90%) achieved in hydrogenation experiments.[8,9] From an analysis of the conformational properties of chirally substituted 1,3-diaminopropanes, it has been argued that with these amino ligands, which have a substitution pattern equivalent to that of skewphos, the twist conformation should be preferred on energetic grounds.[10] For chiral 1,3-diphosphanylpropane chelate cycles, the experimental material available so far[6,9] is not sufficient to deduce any general trends in this respect, nor are reliable force-field calculations available for isolated cycles.[11] In an attempt to create a structural database of chirally substituted 1,3-bis(phosphanyl)propane chelate cycles, with the ultimate aim of deriving a reliable force-field description by global optimization[12] of the relevant force-field parameters, a series of chiral 1,3-bis(phosphanyl)propanes (L_2) has been synthesized. Their rhodium complexes $[L_2Rh(COD)]PF_6$ (**2**) have been prepared and, where possible, structurally characterized as

[a] Anorganisch-Chemisches Institut der Universität Heidelberg, Im Neuenheimer Feld 270, D-69120 Heidelberg, Germany
Fax: (internat.) + 49(0)6221/545707

 © WILEY-VCH Verlag GmbH, D-69451 Weinheim, 1999 1434–1948/99/0303–0405 $ 17.50+.50/0

well. The catalytic activities of these complexes and the associated enantioselectivities have been probed and it has been found that [(**1g**)Rh(COD)]PF_6 [**1g** = $Ph_2PCH_2CH(OH)CH_2P(2\text{-}MeOPh)_2$] permits up to 85% *ee* in the rhodium-mediated hydrogenation of (*Z*)-2-acetamidocinnamic acid (AAC).

Results and Discussion

Ligands

It has been reported that epichlorohydrin $H_2C(O)CHCH_2Cl$ (**A**) permits a simple and fully stereoselective synthesis of chiral tripod ligands $X_2POCH(CH_2PR_2)(CH_2PR'_2)$.[13] The corresponding tripod rhodium compounds, on the other hand, have been shown to be rather sluggish catalysts offering only slight enantiomeric discrimination.[14] Their reduced reactivity and low enantioselectivity has been explained on the basis of the hypothesis that in order to form active catalyst precursors, η^2-diphos species first have to be generated from the η^3-coordinated compounds by dissociation of one of the "legs" of the tripod ligands.[14,15] This hypothesis is well supported by a series of observations made for catalytic systems involving tripod metal entities.[14–17] In the light of this hypothesis, a logical course of action is to probe diphos ligands $HOCH(CH_2PR_2)(CH_2PR'_2)$, which differ from the above tripod ligands simply by the absence of the third oxygen-supported "leg". Such ligands are easily accessible by the same sequence of reactions as that used for the synthesis of the above tripod ligands.

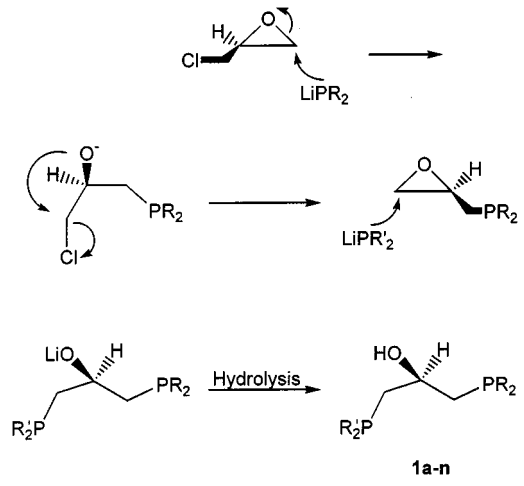

Scheme 1. Reaction scheme

The reaction scheme shown for the consecutive addition of two phosphorus-centred nucleophiles (**1a–1l**) may be adapted to allow the incorporation of sulfur- or nitrogen-centred nucleophiles as well (**1m**, **1n**). Compounds **1** were purified by column chromatography and were obtained as colourless oils of modest to low viscosity. In no case could a crystalline product be obtained. In most cases it proved difficult to completely remove the solvent and successive cycles of freezing and drying had to be applied to overcome this problem. The microanalytical data were in agreement with the assigned constitutions with only a few exceptions (Tables 8 and 11). In these cases, high-resolution mass spectrometry was used as an analytical tool (Tables 8 and 11).

Table 1. Ligands **1a–1n**

	R	R′[a]
1a: (*S*)-	Ph	3,5-Me_2Ph
1b: (*R*)-	*o*-Tol	Ph
1c: (*S*)-	*o*-Tol	DBP
1d: (*S*)-	Ph	Mes
1e: (*S*)-	Mes	DBP
1f: (*R*)-	2-MeOPh	Mes
1g: (*S*)-	Ph	2-MeOPh
1h: (*S*)-	Ph	2-EtPh
1i: (*S*)-	Ph	2-Me_2NPh
1j: (*S*)-	Et	Mes
1k: (*S*)-	Et	*o*-Tol
1l: (*S*)-	Et	2-MeOPh
1m: (*S*)-	Ph	SPh
1n: (±)-	Ph	NPh_2

[a] R′ in PR'_2 for **1a–1l**, donor group for **1m**, **1n**.

The ^{31}P-, ^{13}C-, and ^{1}H-NMR spectra provided further unequivocal evidence for the identity of the compounds (Tables 9, 10, 12, and 13). The assignment of the individual signals was in part based on the observation that chemically different PR_2 groups give rise to ^{31}P resonances in distinct and different ranges [dibenzophospholyl (DBP): δ = −20 to −23; PPh_2: δ = −21 to −25; PEt_2: δ = −26 to −30; $PMes_2$: δ = −30 to −33; $P(C_6H_4OMe)_2$: δ = −41 to −45; $P(o\text{-}Tol)_2$: δ = −44 to −47 (Tables 10 and 13)]. Comparing the whole set of spectra of compounds **1**, assignments based on these shift ranges were thus possible, whereas owing to the narrow range of shifts of specific organic groups, individual assignments of all the ^{13}C and ^{1}H resonances were not possible in all cases. The shifts and patterns observed leave no doubt as to the identity of **1** (Tables 9, 10, 12, and 13). The chirality of **1** gives rise to a range of specific rotations of $|[\alpha]_D^{20}| = 1–79$ (Tables 8 and 11).

With the donor groups $PMes_2/PEt_2$ (**1j**) and $P(o\text{-}Tol)_2/PEt_2$ (**1k**), the synthesis was performed by two alternative routes, as shown for **1j** in Scheme 2.

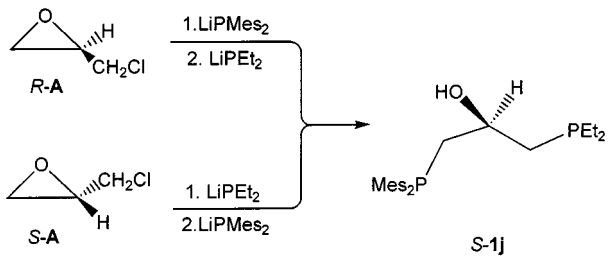

Scheme 2. Alternative syntheses of (*S*)-**1j**

Either (*R*)-**A** was used as the starting compound and the phosphane donors were introduced in the sequence: 1. $PMes_2$, 2. PEt_2, to obtain **1j** [or: 1. $P(o\text{-}Tol)_2$, 2. PEt_2, to produce **1k**], or alternatively (*S*)-**A** was used with the inverse

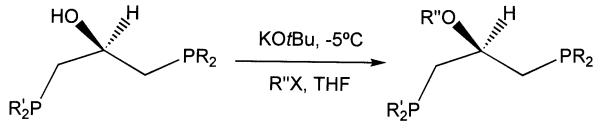

Scheme 3. Synthesis of ether derivatives **1**

sequence of addition. Both reactions lead to the same compound with the same chirality provided they are, as documented,[13,18] fully stereoselective. In line with expectation, the optical rotations of the two pairs of samples prepared by these two routes were in fact equal (**1j**: $[\alpha]_D^{20} = +46.2$, **1k**: $[\alpha]_D^{20} = +15.7$, Table 8).

All of the ligands **1a−1n** contain a hydroxy function. Etherification of this type of function in the presence of phosphane groups may be problematic.[19] For tripod ligands $HOCH_2C(CH_2PPh_2)_3$, a strategy that circumvents the problems caused by the nucleophilicity of the phosphorus functions in the course of a Williamson-type etherification has been developed.[20] The same type of reaction protocol works equally well with the diphos ligands **1**. The compound $Ph_2PCH_2CH(OH)CH_2PPh_2$, prepared by literature methods,[13] reacts with methyl iodide after depro-

Table 2. Ligands **1o−1u**

	R	R′	R′′	X
1o:	Ph	Ph	CH_3	I
1p: (*R*)-	*o*-Tol	Ph	CH_3	I
1q: (*R*)-	*o*-Tol	Ph	$SiMe_3$	Cl
1r: (*R,S*)-	*o*-Tol	Ph	(*S*)-$H_3CCH_2CH(CH_3)CH_2$	OTs
1s: (*S*)-	Ph	2-MeOPh	$SiMe_3$	Cl
1t: (*S,S*)-	Ph	2-MeOPh	(*S*)-$H_3CCH_2CH(CH_3)CH_2$	OTs
1u: (*S*)-	Ph	Mes	$H_2CCH[CH_2]_9$	OTs

Table 3. Synthesis and analytical data of complexes **2**

	R	R′[a]	R′′	yield (%)	MS (FAB) [M^+], [M^+ − COD]	$[\alpha_D^{20}]$	$C_{calcd.}H_{calcd.}P_{calcd.}$ $C_{found}H_{found}P_{found}$	M.p.[f] [°C]
2a: (*S*)-	Ph	3,5-Me_2Ph	H	92	695, 586	8.1 ± 1.5	54.29, 5.91, 11.35 54.57, 5.52, 10.38	167
2b: (*R*)-	*o*-Tol	Ph	H	83	667, 559	−19.0 ± 0.1	54.69, 5.21, 11.44 53.66, 5.69, 10.45	173
2c: (*S*)-	*o*-Tol	DBP	H	86	664, 557	−22.4 ± 1.1	54.83, 4.97, 11.46 55.13, 5.32, 11.10	175 (dec.)
2d: (*S*)-	Ph	Mes	H	93	723, 615	−61.8 ± 0.1	56.69, 5.80, 10.70 55.72, 6.08, 10.16	200
2e: (*S*)-	Mes	DBP	H	95	721, 613	39.2 ± 0.9	52.99, 5.30, 9.76[b] 53.01, 5.30, n.d.	208 (dec.)
2f: (*R*)-	2-MeOPh	Mes	H	74	783, 675	29.2 ± 0.5	52.14, 5.57, 9.17[b] 51.76, 5.63, 8.73	226
2g: (*S*)-	Ph	2-MeOPh	H	84	699, 591	10.7 ± 0.1	52.62, 5.01, 11.00 51.84, 5.10, n.d.	207
2h: (*S*)-	Ph	2-EtPh	H	91	695, 584	12.4 ± 0.1	55.72, 5.52, 11.05 56.47, 6.07, n.d.	140
2i: (*S*)-	Ph	2-Me_2NPh	H	See Experimental Section				
2j: (*S*)-	Et	Mes	H	97	627, 519	8.0 ± 0.1	51.30, 6.52, 12.03 50.83, 6.57, 11.99	136
2k: (*S*)-	Et	*o*Tol	H	88	571, 463	−74.5 ± 2.8	48.62, 5.91, 12.97 48.41, 5.97, 13.05	201
2l: (*S*)-	Et	2-MeOPh	H	81	603, 495	−47.4 ± 2.9	46.54, 5.66, 12.41 46.60, 5.71, n.d.	164 (dec.)
2m: (*S*)-	Ph	SPh	H	77	563, 455	79.1 ± 0.2	49.16, 4.69, 8.74 48.30, 4.71, 7.78	180
2n: (±)-	Ph	NPh_2	H	See Experimental Section				
2o:	Ph	Ph	CH_3	86	653, 545	−	52.13, 4.91, 11.05[c] 51.83, 5.08, n.d.	206 (dec.)
2p: (*R*)-	*o*-Tol	Ph	CH_3	81	681, 572	10.4 ± 1.4	55.22, 5.37, 11.24 53.41, 5.33, n.d.	174
2q: (*R*)-	*o*-Tol	Ph	$SiMe_3$	83	739, 631	18.6 ± 1.6	54.30, 5.71, 10.50 52.16, 5.79, n.d.	173
2r: (*R,S*)-	*o*-Tol	Ph	X[d]	89	737, 629	−5.8 ± 0.1	57.15, 5.94, 10.53 56.69, 5.87, n.d.	210 (dec.)
2s: (*S*)-	Ph	2-MeOPh	$SiMe_3$	79	771, 663	−7.9 ± 1.1	52.41, 5.50, 11.00 52.12, 5.51, n.d.	208 (dec.)
2t: (*S,S*)-	Ph	2-MeOPh	X[d]	87	769, 661	11.6 ± 0.5	55.15, 5.73, 10.16 54.87, 5.70, n.d.	134
2u: (*S*)-	Ph	Mes	Y[e]	46	875, 763	−39.2 ± 1.5	61.18, 6.91, 9.10 58.52, 7.19, n.d	180 (dec.)
2v:	Ph	Ph	H	89	639, 531	−	53.56, 4.88, 11.85 53.16, 5.14, 11.63	193
2w: (*R*)-	*p*-Tol	Ph	H	74	667, 559	−5.4 ± 0.9	54.69, 5.21, 11.44 53.92, 5.48, 10.67	188

[a] R′ in PR'_2 for **2a−2l** and **2o−2w**, donor group for **2m**, **2n**. − [b] = M · CH_2Cl_2. − [c] = M · 0.5 CH_2Cl_2. − [d] X = (*S*)-$H_3CCH_2CH(CH_3)CH_2$. − [e] Y = $H_2CCH[CH_2]_9$. − [f] dec. = decomposition.

tonation with KO*t*Bu at temperatures below 20°C to produce **1o**. In the same way, **1b** is transformed into **1p**. Stringent temperature control is necessary to avoid alkylation at the phosphorus atom.[20] With **1g** as the starting material, however, exclusive methylation at the oxygen position with methyl iodide proved impossible, even under these controlled conditions. The increased nucleophilicity of the $(2\text{-MeOPh})_2P$ function leads to partial quaternization of this phosphorus centre during the course of the reaction. On the other hand, etherification by the tosylate H_3CCH_2-$CH(CH_3)CH_2OTs$ could be achieved both for **1b** (→ **1r**) and for **1g** (→ **1t**). Silylation (**1b** → **1q**, **1g** → **1s**) did not present any problems of this kind.

With longer-chain tosylates, problems tend to arise in the separation of the ligands from the long-chain alcohols. Thus, when **1d** was treated with $H_2C{=}CH(CH_2)_9OTs$, the corresponding ether derivative (**1u**) was obtained, which could, however, not be obtained in an analytically pure state as such (Table 11), but was unequivocally characterized by the data obtained for its coordinated derivative **2u** (Table 3).

Coordination Compounds

Ligands **1** react with $[Rh(COD)Cl]_2$ under standard conditions to give the coordination compounds **2** [(**1a**–**u**)Rh-(COD)]PF_6.

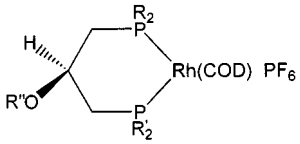

Scheme 4. Constitution of compounds **2**

The labelling scheme used is such that coordination compound **2**"label" contains ligand **1**"label". Coordination compounds **2v** (R = R′ = Ph) and **2w** (R = *p*-Tol, R′ = Ph) were obtained from the appropriate ligands, the preparation of which has been described previously.[13] Compounds **2** were obtained as orange, microcrystalline solids.

The identities of compounds **2** were evident from their analytical data (Table 3), as well as from several X-ray analyses (see below). Elemental analyses, as well as the mass numbers as determined by FAB mass spectrometry, were in agreement with the constitutions as given. The optical rotations of the chiral compounds (all compounds except **2o**, **2v**) were found to be in the absolute range $|[\alpha]_D^{20}| = 5.4-79$ (Table 3).

The ^{1}H-NMR spectra are cumbersome to interpret. In most cases, broad signals are found at room temperature and the spectra are strongly temperature-dependent, indicating a dynamic behaviour of the chelate cycles. This is clearly borne out by analysis of the ^{31}P-NMR spectra (see

Table 4. $^{31}P\{^1H\}$-NMR data of complexes **2**[a]

	R	R′[b]	*T* [K]	PR_2 δ ($^1J_{PRh}$, $^2J_{PP}$)		PR'_2 δ ($^1J_{PRh}$, $^2J_{PP}$)
2a: (*S*)-	Ph	3,5-Me_2Ph	298	15.6 (141, 44)		16.8 (143, 44)
2b: (*R*)-	*o*-Tol	Ph	388[c]	15.9 (145, 43)		19.3 (141, 43)
2c: (*S*)-	*o*-Tol	DBP	403[c]	14.3 (142, 46)		18.3 (br) (140, 46)
2d: (*S*)-	Ph	Mes	340[c]	8.0 (br) (148, 36)		−2.4 (133, 37)
			298	I) 7.0 (148, 36)		I) −2.2 (133, 37)
				II) 11.2 (150, 36)		II) −4.5 (132, 36)[d]
					I:II = 4.5:1	
2e: (*S*)-	Mes	DBP	298[e]	I) −0.7 (135, 37)		I) 7.0 (144, 37)
				II) 0.2		II) 11.8 (146, 39)[d]
					I:II = 7:1	
2f: (*R*)-	2-MeOPh	Mes	298[e]	I) 12.3 (151, 34)		I) −6.7 (34, 133)
				II) 8.5 (149, 34)		II) −3.5 (35, 134)[d]
					I:II = 1:3	
2g: (*S*)-	Ph	2-MeOPh	378[c]	12.6 (142, 46)		16.5 (145, 46)
2h: (*S*)-	Ph	2-EtPh	388[c]	18.5 (br)		16.1 (145, 43)
2j: (*S*)-	Et	Mes	298	I) 2.9 (35, 141)		I) −3.0 (37, 136)
				II) 7.6 (36, 140)		II) −2.0 (37, 135)[d]
					I:II = 7:1	
2k: (*S*)-	Et	*o*-Tol	298	22.7 (br)		8.0 (br)
2l: (*S*)-	Et	2-MeOPh	298[e]	19.4 (br)		8.7 (br)
2m: (*S*)-	Ph	SPh	298	18.1 (143)		
2o:	Ph	Ph	298	15.1 (145.8)		
2p: (*R*)-	*o*-Tol	Ph	298	10.0−20.0 (br)		
2q: (*R*)-	*o*-Tol	Ph	298	5.0−10.0 (br)		
2r: (*R,S*)-	*o*-Tol	Ph	298	11.0−19.3 (br)		
2s: (*S*)-	2-MeOPh	Ph	368[c]	17.2 (46, 145)		13.3 (46, 142)
2t: (*S,S*)-	2-MeOPh	Ph	298	9.0−17.9 (br)		
2u: (*S*)-	Ph	Mes	298	I) 7.6 (147, 37)		I) −3.3 (134, 37)
				II) 11.1 (150, 37)		II) −2.9[d]
					I:II = 8:1	
2v:	Ph	Ph	298	15.8 (144)		
2w: (*R*)-	*p*-Tol	Ph	298	14.5 (45, 141)		18.8 (45, 144)

[a] br = broad; for complexes **2i**, **2n** see Experimental Section. – [b] R′ in PR'_2 for **2a**–**2l** and **2o**–**2w**, donor group for **2m**. – [c] High temperature limit. – [d] I, II: two conformational isomers at the temperature of observation. – [e] Decomposition upon heating.

below). Individual assignment of groups of signals is nevertheless possible in the ^1H- (Table 14) as well as in the ^{13}C-NMR spectra (Table 15). Full interpretation of the spectra would, however, require an intricate analysis of the dynamic behaviour. The spectra of **2a**, **2m**, **2o**, **2v**, **2w** are comparatively sharp at room temperature and indicate the presence of one single species, at least over the time average. Sharp signals are also observed for compounds **2d−f**, **2j**, and **2u**, which contain $PMes_2$ groups. For these species, however, the presence of two different conformers (see below) leads to an overlap of signals, which hampers the unambiguous assignment of their ^1H and ^{13}C data.

The most clear-cut information is provided by the ^{31}P-NMR spectra. They are in agreement with the given constitutions in that they show the appropriate signals for each of the differently substituted PR_2 entities within the chelate cycle (Table 4). The signal pattern characteristic for each of the phosphorus nuclei consists of a doublet of doublets with $^1J_{PRh} \approx 140$ Hz, $^2J_{PP} \approx 40$ Hz (Table 4). There are only two compounds where the PR_2 groups are equal (**2o**, **2v**), and only one kind of phosphorus signal (doublet, $^1J_{PRh} \approx 145$ Hz) is observed in these cases at 293 K (Table 4).

The dynamic behaviour of the compounds is in some cases already apparent at or above room temperature, and is a rather general phenomenon. In the cases of **2d−f**, **2j**, and **2u**, which contain $PMes_2$ groups, the behaviour is static already at room temperature, where two different conformers give rise to two sets of signals. Two conformers are sometimes observed for compounds **2** in the solid state as well (see below).

The kind of dynamic behaviour is not always directly evident from the spectra, since there are a number of conceivable dynamic processes. In some cases, hindered rotation of *ortho*-substituted aryl groups as well as conformational changes of the chelate cycles seem to be simultaneously operative in the same system. Not all of the dynamic processes have yet been delineated, hence the types of process will be described here only for especially clear-cut cases.

With **2b**, the only dynamic process observed on the timescale of the experiment is the hindered rotation of the *ortho*-tolyl groups of the P(*o*-Tol)$_2$ moiety. At 273 K, broad multiplets are observed (Figure 1). Upon heating, one clear doublet of doublets structure is observed (Figure 1), which indicates that one of the phosphorus nuclei is not influenced by a change of the environment. The signal of the other phosphorus atom, however, is completely broadened into the baseline at 313 K; its signal starts to reappear at 328 K and a clear doublet of doublets pattern is observed at 388 K. Above this temperature, the compound starts to decompose and so the high-temperature limit can only be approached (Figure 1). The structure of the new signal observed at 388 K leaves no doubt that it has to be assigned to the second phosphorus atom ($^1J_{PRh} = 145$ Hz, $^2J_{PP} = 43$ Hz).

The signals also sharpen at temperatures below 273 K, giving rise to two patterns, each composed of two doublet of doublets structures. The innermost pattern (Figure 1, 213 K) corresponds to one set of two chemically different phosphorus nuclei, and the outer one characterizes another pair of chemically different phosphorus atoms. The coherence of the outer set of signals is evident from PPCOSY experiments (Figure 2). The inner set of signals is of higher order, and its coherence is clear from the type of pattern as well as from the coupling constants.

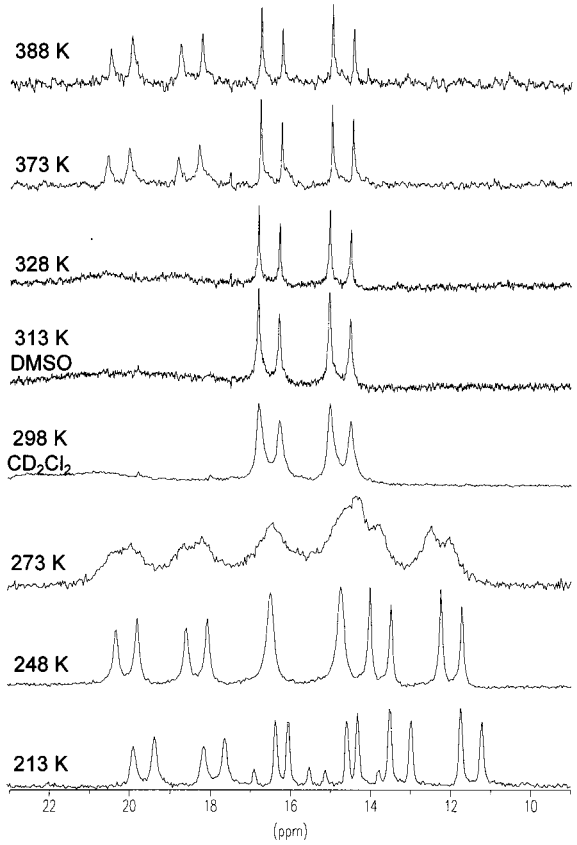

Figure 1. Temperature dependence of the $^{31}P\{1H\}$-NMR spectrum of **2b**

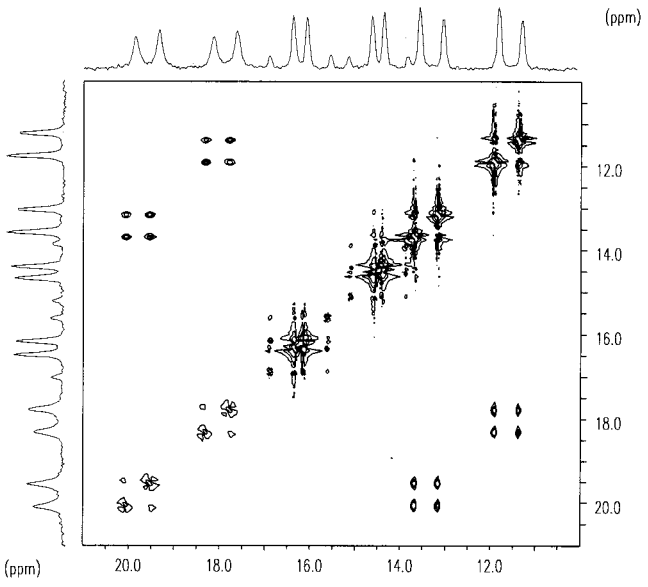

Figure 2. ^{31}P-^{31}P COSY experiment on **2b** at 213 K

These observations can be interpreted as follows. The tolyl groups of the P(*o*-Tol)$_2$ fragment of the compound are fixed in two different positions at the low temperature limit and are, focusing only on a single P(*o*-Tol)$_2$ group, mirror images of one another. Either the left-hand aryl group has its methyl substituent pointing forward while the right-hand group has it pointing backwards (Figure 3), or vice versa. Thus, there are two conformers present at the low-temperature limit. Evidently, the conformation of the chelate cycle is either still fully dynamic at this temperature, or the different conformations which it might adopt (chair, twist) do not significantly influence the phosphorus resonances.

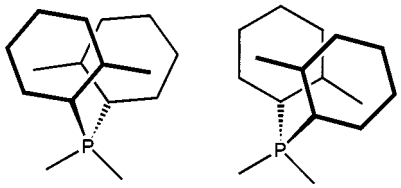

Figure 3. Conformations of the P(*o*-Tol)$_2$ fragment

The conformational enantiomerization of the P(*o*-Tol)$_2$ group, which is the rationale for the fact that two different species are observed at the low-temperature limit, also accounts for the changes observed in the spectra at higher temperatures. Just above 273 K (Figure 1), a clear doublet of doublets structure evolves for one of the constitutionally different PR_2 groups. The second one is not observable at all. This indicates that the environment of the "unobservable" phosphorus atom changes at such a rate that no signal is observed. At higher temperatures, this change speeds up and the signal appears as a doublet of doublets. The change of environment is due to the enantiomerization of the P(*o*-Tol)$_2$ conformation. The phosphorus atom of the P(*o*-Tol)$_2$ group itself does not take much notice of this conformational change, whereas the PPh_2 "spectator" group well feels it.

The validity of the above interpretation is corroborated by the observation of analogous behaviour in a case where there is no doubt as to which phosphorus signal is from which group. The ^{31}P-NMR spectra of the whole series of compounds $H_3C(CH_2PPh_2)_n[CH_2P(o\text{-}Tol)_2]_{3-n}Mo(CO)_3$ have been thoroughly analysed with regard to their dynamic behaviour.[21] The conformational enantiomerization (see above) of the P(*o*-Tol)$_2$ groups lies at the basis of the dynamic processes observed for these species. For $H_3C(CH_2PPh_2)_2[CH_2P(o\text{-}Tol)_2]Mo(CO)_3$, it has been found that the signal of the phosphorus atom of the P(*o*-Tol)$_2$ group is undisturbed by the enantiomerization of the P(*o*-Tol)$_2$ conformation, while the phosphorus nuclei at the two spectator PPh_2 groups are strongly influenced.[21]

Compound **2c** is an analogue of **2b**, the only difference being that the phenyl groups of the PPh_2 moiety of **2b** are linked by a carbon−carbon bond in its dibenzophosphole donor group. The dynamic behaviour of **2c** is found to be qualitatively analogous to that of **2b** in the high-temperature range (Figure 4). In the low-temperature range between 298 K and 218 K, the behaviour is again similar with the signals of two different species gradually evolving. At the lowest accessible temperature (185 K), however, there is seemingly only one species. This implies that one of the diastereomers generated by the conformational isomerism of the P(*o*-Tol)$_2$ group is decidedly more stable than its epimeric form.

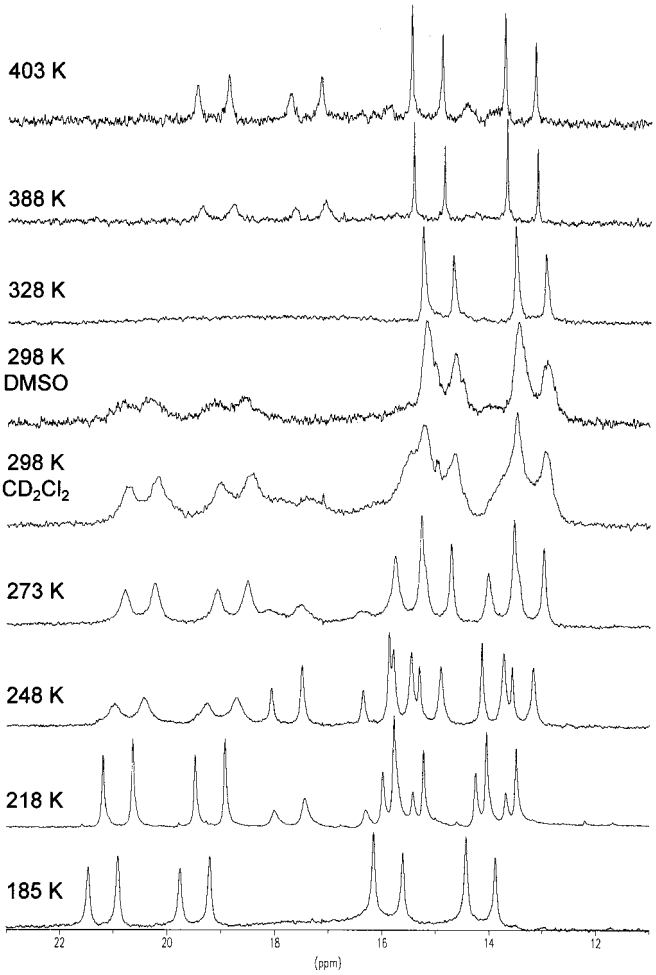

Figure 4. Temperature dependence of the $^{31}P\{^1H\}$-NMR spectrum of **2c**

X-ray Analyses

The kind of dynamic behaviour indicated by the NMR observations has not yet been fully delineated for all compounds **2**. It will in part be associated with the conformational flexibility of the chelate cycles, and the X-ray data obtained for **2** (Table 5) clearly show that these can adopt chair as well as twist conformations.

Considering structurally equivalent moieties, the scalar properties (distances, angles) are rather similar for the whole group of compounds (Table 6). The real difference between the compounds is apparent from the torsion angles (Table 5). There are five independent molecules that adopt chair conformations (Table 5), with the crystal structure of **2b** containing two crystallographically independent molecules of this type. The torsion angles within this group of

conformationally similar molecules are not too dissimilar within each set of conformationally equivalent groups (cf. columns φ_{2345}, φ_{6543} in Table 5; these angles should be equal in size but opposite in sign for a mirror-symmetric chair. The signs of the torsion angles of **2c** are the opposite of those of **2b**; this is not a physically relevant difference but arises because of the priority rules used to assign chirality). The different conformational classes are most clearly apparent from the pseudo torsion angle φ_{3265} (Table 5), which is close to zero for the chair conformations and +/−51−56° for the δ or λ conformations (Table 5).

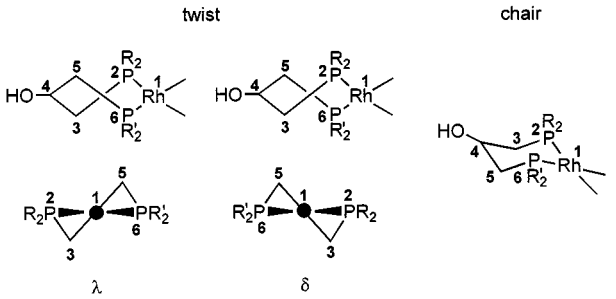

Figure 5. Schematic illustration of the conformations adopted by the chelate cycles in **2**

To illustrate the twist conformation the structures of the δ and λ conformations, both of which are found in the crystal of **2d**, are illustrated in Figure 6. The two molecules are conformational diastereomers. Even though the chirality defined by the substitution pattern at the ligand is the same for both molecules, the additional chirality induced by the twist of the chelate cycle is opposite in sense for the two

Table 5. Torsion angles for the chelate cycles of compounds **2**[a]

	R	R′	conf.	φ_{1234}	φ_{1654}	φ_{2345}	φ_{6543}	φ_{6123}	φ_{2165}	φ_{3265}
2v	Ph	Ph	chair	52	−57	−74	82	−32	32	1
2o	Ph	Ph	chair	64.9	−58.7	−75.3	71.3	−42.2	40.5	−2.5
2b	Ph	*o*-Tol	chair	48.6	−51.9	−73.9	74.6	−23.0	24.6	1.3
	Ph	*o*-Tol	chair	57.8	−58.8	−74.6	74.5	−36.0	36.6	0.5
2d	Ph	Mes	δ	−73.9	−69.3	40.4	32.1	28.2	28.1	54.3
	Ph	Mes	λ	67.2	79.9	−20.7	−53.7	−30.8	−24.9	−54.3
2g	Ph	2-MeOPh	δ	−74.1	−62.8	45.5	22.8	27.3	27.8	51.6
	Ph	2-MeOPh	λ	65.3	74.2	−24.1	−45.8	−27.9	−25.6	−51.2
2f	Mes	2-MeOPh	δ	−72.6	−72.5	30.9	42.9	33.7	23.6	55.6
	Mes	2-MeOPh	λ	79.5	65.7	−46.7	−28.1	−30.9	−23.9	−54.6
2e	Mes	DBP	δ	−81.6	−59.5	42.4	28.5	37.2	15.9	51.8
2c	*o*-Tol	DBP	chair	−53.9	45.9	74.2	−71.2	27.1	−23.2	3.5

[a] The numbering scheme adopted refers to Figure 5 throughout and is different from the schemes used to label individual atoms in the deposited data.[36]

Table 6. Distances and angles in compounds **2**[a]

	R R′	conf.	Rh−PR_2 Rh−PR'_2	Rh−C_{COD} (R)[b]	Rh−C_{COD} (R′)[b]	PR_2−C3 PR'_2−C5	C4−C3 C4−C5	PRhP
2v[c]	Ph	chair	226.5(4)					91.2(2)
	Ph		228.2(5)					
2o	Ph	chair	230.6(2)	226.2(6)	222.9(6)	183.9(5)	152.5(8)	88.6(5)
	Ph		229.6(6)	223.6(5)	222.6(6)	184.0(5)	153.1(7)	
2b	Ph	chair	230.0(2)	225.2(7)	230.6(7)	183.2(7)	154.7(11)	91.6(1)
	o-Tol		232.8(2)	225.4(8)	224.8(8)	184.7(7)	152.0(10)	
	Ph	chair	231.1(2)	228.2(8)	226.0(9)	182.8(9)	151.7(12)	89.6(1)
	o-Tol		232.2(2)	225.4(8)	222.9(8)	184.5(7)	150.4(12)	
2d	Ph	δ	230.4(2)	222.4(10)	225.8(8)	181.3(9)	153.6(13)	87.8(1)
	Mes		233.4(2)	223.1(9)	226.1(9)	184.7(10)	151.6(13)	
	Ph	λ	229.6(2)	219.4(9)	225.4(9)	186.9(8)	151.5(13)	88.3(1)
	Mes		232.1(2)	226.3(8)	219.8(8)	184.9(9)	157.8(13)	
2g	Ph	δ	228.8(3)	223.9(8)	228.0(11)	182.2(7)	154.6(13)	87.7(1)
	2-MeOPh		231.3(2)	222.7(9)	223.9(10)	183.0(11)	156.2(16)	
	Ph	λ	229.3(2)	224.3(11)	223.3(13)	184.5(7)	153.6(11)	87.7(1)
	2-MeOPh		231.4(2)	222.7(9)	225.7(11)	185.4(9)	148.0(13)	
2f	Mes	δ	235.6(3)	217.9(17)	219.5(15)	184.5(2)	161.3(2)	87.7(1)
	2-MeOPh		234.6(4)	225.1(15)	229.1(12)	180.8(2)	153.7(2)	
	Mes	λ	231.2(4)	228.3(18)	225.2(16)	185.6(13)	149.8(2)	88.9(1)
	2-MeOPh		230.1(4)	225.2(13)	221.6(14)	182.9(12)	148.3(2)	
2e	Mes	δ	232.0(1)	225.3(3)	224.6(3)	186.4(3)	153.5(4)	87.2(3)
	DBP		229.9(1)	224.1(3)	225.8(3)	184.0(4)	153.7(5)	
2c	*o*-Tol	chair	231.3(1)	223.9(5)	229.5(4)	185.5(4)	152.0(6)	91.3(4)
	DBP		227.2(1)	226.4(4)	224.0(4)	183.4(4)	152.8(6)	

[a] The numbering scheme adopted refers to Figure 5 throughout and is different from the schemes used to label individual atoms in the deposited data.[36] − [b] C_{COD} *cis* to PR_2 (PR'_2). − [c] The structure of **2v** is rather inaccurate, disorder is observed for the COD ligand and for the aryl substituents of one of the PPh_2 groups. Only items involving solely P and Rh are therefore given in the table. The overall geometry is nevertheless clearly evident, as is the chair-type conformation of the chelate cycle (Table 5).

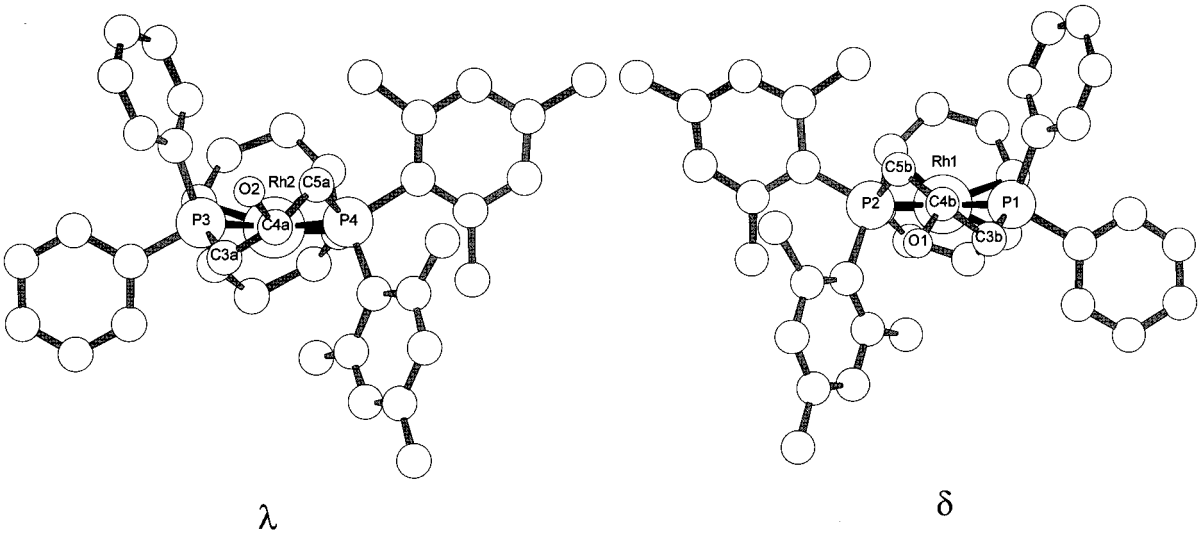

Figure 6. Conformations of the cation of **2d** as observed in the solid state; the numbering scheme refers to Figure 5; the designators *a* and *b* are used to differentiate between the two different molecules in the crystal of **2d**

species. It appears that with the substituents used, enantioselective discrimination is not sufficient to make one of the ring conformations much more stable than the other. The ^{31}P-NMR spectra of **2d** (see above, Table 4) show that two conformers are also present in solution at room temperature. In contrast to **2b**, **2c** (see above), it is not clear, however, whether the conformational isomerism observed in solution is due to an inversion of the ring conformation or to the hindered rotation of the mesityl groups.

The results presented in Table 5 suggest that sterically more demanding substituents at the phosphorus centres favour twist conformations. Chair conformations are found for **2b**, **2c**, **2o**, **2v**, and their overall geometry is illustrated for **2b** (Figure 7). Only one of the two geometrically almost equivalent independent molecules in the crystal of **2b** is shown in Figure 7. Despite the fact that **2b** adopts a chair conformation in the solid state, two conformers are observed in solution at low temperatures, which are attributed to a rotational isomerism of the P(*o*-Tol)$_2$ group (see above). In the crystal, the P(*o*-Tol)$_2$ groups of the two independent molecules adopt the same orientation.

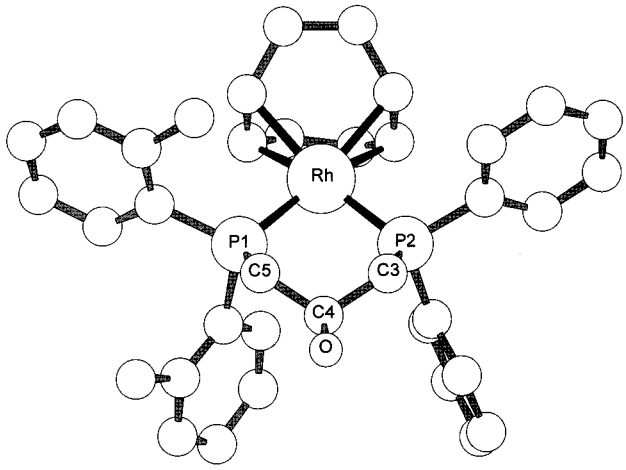

Figure 7. Conformation of the cation of **2b** as observed in the solid state; the numbering scheme refers to Figure 5

Catalysis

Compounds **2** act as precatalysts in the catalytic hydrogenation of (*Z*)-2-acetamidocinnamic acid (AAC). Table 7 shows the relative efficiencies of the various compounds **2**, together with the *ee* values observed in each case. The highest rate is observed for **2v**, i.e. for the sterically least demanding ligand, $Ph_2PCH_2CH(OH)CH_2PPh_2$, of the series. The activity of **2v** is similar to that observed for $[Ph_2PCH_2C(CH_3)_2CH_2PPh_2]Rh(COD)^+$.[22] The reactivity is not significantly reduced by *para* substitution of one of the PPh_2 groups [P(*p*-Tol)$_2$, **2w**], nor by *meta* substitution [P(*m*-Xyl)$_2$, **2a**], see Table 7. The enantiodiscriminating influence of this type of substitution is also low (*ee* = 3% and 6%, respectively). Replacing one of the PPh_2 groups by a P(*o*-Tol)$_2$ group (**2b**) has virtually no effect on the reactivity, but the enantiomeric excess is found to rise to 36% (*S*) at 20°C, 40% at 50°C, and 49% at 30 bar, 25°C. To examine the influence of the OH substituent on the backbone of the ligand, *O*-alkylated and *O*-silylated derivatives of **2b** were analysed. It was found that **2p** (substituent OCH_3), **2q** (substituent $OSiMe_3$), and **2r** [substituent (*S*)-H_3CCH_2-$CH(CH_3)CH_2O$] required longer reaction times in order to reach full conversion (Table 7). The enantiomeric excess, however, proved to be almost independent of this type of substitution (Table 7).[22]

Replacing the PPh_2 group in **2b** by a DBP group (**2c**) greatly reduces the reactivity. The enantioselectivity becomes inverted such that the product is of (*R*) configuration. Increasing either the temperature or the pressure results in reduced selectivity. Replacing one of the PPh_2 groups in **2v** by an SPh donor (**2m**) also reduces the reactivity, with the observed *ee* value lying at the lower end of the range. Although the large difference between the properties

Table 7. Catalytic activity of compounds **2** in the hydrogenation of (*Z*)-2-acetamidocinnamic acid[a]

	1 bar								30 bar[b]		
	0°C			20°C			50°C			25°C	
	t	yield (%)	*ee*	*t*	yield (%)	*ee*	*t*	yield (%)	*ee*	*t*	yield (%)	*ee*
2v				20 min	100	0						
2w				30 min	100	3 (*R*)						
2a				25 min	100	6 (*R*)	15 min	100	0			
2b				30 min	100	36 (*S*)	25 min	100	40 (*S*)	48 h	100	49(*S*)
2p				2.5 h	100	38 (*S*)						
2q				5 h	100	35 (*S*)						
2r				22 h	100	40 (*S*)						
2c				7 h	100	23 (*R*)	1 h	100	20 (*R*)	48 h	30	4 (*S*)
2m				10 h	100	14(*R*)						
2d				4 d	< 10	n.d.	5 d	16	31 (*R*)	60 h	52	40 (*R*)
2u										5 d	100	40 (*R*)
2e										48 h	12	n.d.
										5 d	90	64 (*R*)
2h	4 h	100	56 (*R*)	2 h	100	48 (*R*)				16 h	100	62 (*R*)
2g				40 h	100	77 (*S*)				48 h	100	67 (*S*)
	2.5 h[c]	100	85 (*S*)	1 h[c]	100	77 (*S*)						
2s				2 h[c]	100	77 (*S*)						
2t	20 h[c]	100	82 (*S*)	2.5 h[c]	100	79 (*S*)						
2f							4 d	< 10	n.d.	5 d	90	64 (*S*)

[a] 1 mol-% catalyst. – [b] For the high-pressure experiments the reaction time was set to the values given and thus has no immediate relation to the reactivity of the catalyst. – [c] 4 mol-% catalyst.

of the donor groups PPh_2 and SPh might be expected to increase enantiomeric discrimination, this expectation is counterbalanced by the fact that the reaction "pocket" accessible to the substrate with the SPh substituent will be larger than that formed by a PPh_2 substituent. Moreover, the coordinated sulfur centre is itself a centre of chirality, the configuration of which could be such as to counteract enantioselectivity.

When one of the PPh_2 groups in **2v** is replaced by a $PMes_2$ group (**2d**), the reactivity is drastically reduced, such that complete conversion could not be achieved under any of the conditions employed (Table 7). Enantioselectivity leading to favoured formation of the (*R*) product is found. Etherification of the OH position (**2u**) again has no significant influence. Replacing the PPh_2 group of **2d** by DBP (**2e**) results in reduced reactivity, but the enantiomeric excess is found to increase to 64% (*R*).

The results of the experiments described so far indicate that in order to obtain sufficient reactivity, a low degree of substitution at the PR_2 entities is favourable. With regard to the enantiomeric excess, it appears that *ortho* substitution of the aryl groups is effective. Etherification at the OH position of the ligands does not appear to have strong influence on the *ee*, but it is found to reduce the reactivity.

With these findings in mind, **2h**, the ethyl-substituted analogue of **2b**, was prepared and screened for its catalytic activity. The reactivity was found to be somewhat lower than that observed with **2b**, but higher enantioselectivity was achieved, rising to 62% *ee* at 30 bar (Table 7). Replacing the ethyl substituents in **2h** by methoxy groups (**2g**) reduces the reactivity, but increases selectivity (Table 7); 77% *ee* (*S*) is observed at 20°C, 1 bar H_2. Increasing the pressure reduces the selectivity to 67% (*S*) at 30 bar H_2. Reducing the temperature to 0°C and compensating for the reduced reactivity by using 4 mol-% catalyst instead of the standard 1 mol-% leads to quantitative conversion in less than 3 h, with an *ee* of 85% (*S*) (Table 7). While enantioselectivities much higher than this have been observed with analogous rhodium complexes derived from five- or seven-membered chelate ligands, to the best of our knowledge there has only been one report to date where a six-membered chelate cycle has led to an *ee* in excess of 80%. The corresponding ligand was skewphos, $Ph_2PCH(CH_3)CH_2CH(CH_3)PPh_2$, which contains two chiral carbon centres in its backbone. On the other hand, the efficiency of *ortho*-alkyloxy substitution in phosphorus-bound aryl groups with regard to enantiomeric discrimination has been known for a long time.[23] In **2g**, both effects, i.e. the skew of the chelate cycle and the activity of the methoxy substituent, may lie at the basis of its enantioselectivity. Further modifications of **2g** by either etherification of its OH group (**2s**, **2t**) or by replacing the PPh_2 group by a $PMes_2$ group (**2f**) did not increase enantioselectivity, but reduced the reactivity to varying extents (Table 7).

Conclusion

The following conclusions can be drawn from the results presented in this paper:

1. Enantiomerically pure chelate ligands $L_2 = XCH_2CHOHCH_2Y$ are easily accessible for a broad range of donor groups X and Y by a two-step synthesis starting from epichlorohydrin. Under specialized conditions, ether derivatives of L_2, $XCH_2CHORCH_2Y$ may be prepared, even with X, Y = PR_2.

2. The chelate cycles in $L_2Rh(COD)^+$ may adopt twist or chair conformations with dynamic equilibria between the different conformations being operative in solution.

3. Compounds $L_2Rh(COD)^+$ act as precatalysts for the homogeneous hydrogenation of AAC. Depending on the nature of the donor groups X and Y, *ee* values of up to 85% can be achieved.

Table 8. Synthesis and analytical data of ligands **1a−1n**

	A[a]	H-Nuc^1 (*t*) H-Nuc^2 (*t*)	eluent (R_f)	yield (%)	α_D^{20}	MS (*m*/*z*) [M^+][M^+ − Frag.]	$C_{calcd.}H_{calcd.}$ $C_{found}H_{found}$	HR-MS $M^+_{calcd./found}$
1a	(*S*)-	$HPPh_2$ (0.5 h) P(*m*-Xylyl)$_2$ (1.5 h)	PE/Et_2O 2:1 (0.28)	82	0.8 ± 0.2	484 407 [−C_6H_5]	76.84, 7.07 75.44, 7.35	
1b	(*S*)-	HP(*o*-Tol)$_2$ (1.5 h) $HPPh_2$ (2 h)	PE/Et_2O 2:1 (0.31)	77	−21.6 ± 3.2	456 379 [−C_6H_5]	76.30, 6.62 76.15, 6.98.	
1c	(*S*)-	HP(*o*-Tol)$_2$ (0.5 h) DBPH (2 h)	PE/Et_2O 3:1 (0.30)	86	−38.7 ± 0.9	454 363 [−$C_6H_4CH_3$]	76.64, 6.21 75.05, 6.46	
1d	(*S*)-	$HPPh_2$ (0.5 h) $HPMes_2$ (1.5 h)	PE/Et_2O 2:1 (0.25)	70	79.3 ± 0.2	512 393 [−C_9H_{11}]	77.32, 7.47 76.55, 7.77	
1e	(*S*)-	$HPMes_2$ (0.5 h) DBPH (2 h)	PE/Et_2O 3:1 (0.28)	56	−92.9 ± 0.7	510 391 [−C_9H_{11}]	77.63, 7.11 77.90, 7.50	
1f	(*R*)-	$HPMes_2$ (0.5 h) HP(2-MeOPh)$_2$ (16 h)	PE/Et_2O 2:1 (0.15)	37	−37.4 ± 0.7	572 453 [−C_9H_{11}]	73.41, 7.39 70.16, 7.56	572.26093 572.26226
1g	(*S*)-	$HPPh_2$ (0.5 h) HP(2-MeOPh)$_2$ (16 h)	PE/Et_2O 1:2 (0.26)	51	3.9 ± 0.2	488 411[−C_6H_5]	71.30, 6.19 69.79, 6.33	488.16702 488.16710
1h	(*S*)-	$HPPh_2$ (2 h) HP(2-EtPh)$_2$ (2 h)	PE/Et_2O 4:1 (0.24)	71	2.9 ± 0.4	484 379 [−C_6H_4Et]	76.84, 7.07 75.21, 7.10	484.20850 484.20882
1i	(*S*)-	$HPPh_2$ (1 h) HP(2-Me_2NPh)$_2$ (16 h)	PE/Et_2O 3:2 (0.31)	53	−6.8 ± 0.4	514 394 [−$C_6H_4NMe_2$]	72.36, 7.05 72.01, 7.01	
1j	(*S*)-	$HPEt_2$ (0.5 h) $HPMes_2$ (1.5 h)	PE/Et_2O 1:2 (0.24)	67	46.2 ± 0.2	416	72.09, 9.20	
1j	(*R*)-	$HPMes_2$ (0.5 h) $HPEt_2$ (1.5 h)	PE/Et_2O 1:2 (0.24)	64		387 [−C_2H_5]	71.43, 9.08	
1k	(*S*)-	$HPEt_2$ (0.5 h) HP(*o*-Tol)$_2$ (2 h)	PE/Et_2O 1:2 (0.24)	57	15.7 ± 0.5	360	69.98, 8.39	360.17719
1k	(*R*)-	HP(*o*-Tol)$_2$ (0.5 h) $HPEt_2$ (1.5 h)	PE/Et_2O 1:2 (0.24)	63		331 [−C_2H_5]	66.42, 8.71	360.17496
1l	(*S*)-	$HPEt_2$ HP(2-MeOPh)$_2$	PE → Et_2O (0.30, Et_2O)	68	0.8 ± 0.2	393 364 [−C_2H_5]	−	−
1m	(*S*)-	$HPPh_2$ HSPh	PE/Et_2O 1:1 (0.39)	84	−29.0 ± 0.2	352 275 [−C_6H_5]	71.57, 6.01 71.66, 6.25	
1n	(±)-	$HPPh_2$ $HNPh_2$	PE/Et_2O 1:2 (0.44)[b]	80	−	411 334 [−C_6H_5]	78.80, 6.37 78.67, 6.65	

[a] Configuration of epichlorohydrin (**A**). − [b] Solid phase for chromatography Al_2O_3 (neutral).

Table 9. ^{1}H-NMR data of ligands **1a−1n**[a]

	R	R′[a]	CH_2PR_2 δ, ($^2J_{HH}$, $^3J_{HH}$)	$CH_2PR'_2$ δ, ($^2J_{HH}$, $^3J_{HH}$)	C*H*−O δ	H_{Ar} δ	aryl subst. δ	other δ
1a: (*S*)-	Ph	3,5-Me_2Ph	2.5−2.7		3.9	7.0−7.5	2.4	
1b: (*R*)-	*o*-Tol	Ph	2.3−2.7		3.9	7.1−7.55	2.46	
1c: (*S*)-	*o*-Tol	DBP	2.2−2.6		4.0	7.1−7.9	2.38	
1d: (*S*)-	Ph	Mes	2.7−2.85 [3 H]	3.2 (13.5, 3.0) [1 H]	3.7	6.8 (Mes) 7.3−7.5	2.3	
1e: (*S*)-	Mes	DBP	3.05 (13.3, 3.1) [1 H]	2.7−2.8 [3 H]	3.82	6.9 (Mes) 7.4−8.0	2.1−2.4	
1f: (*R*)-	2-MeOPh	Mes	2.4−2.7 [3 H]	2.96 (13.7, 3.8) [1 H]	3.7	6.8−7.5	2.25, 3.76 (OMe)	
1g: (*S*)-	Ph	2-MeOPh	2.25−2.65		3.92	6.8−7.5	3.70	2.83 (OH)
1h: (*S*)-	Ph	2-EtPh	2.5−2.75		4.0	7.3−7.6	1.3, 3.0	
1i: (*S*)-	Ph	2-Me_2NPh	2.1−2.5		3.65	6.9−7.45	2.6, 2.8	
1j: (*S*)-	Et	Mes	1.75 [2 H] 2.4−2.7 [2 H]	2.74 3.0 (12.0, 3.4) [1 H]	3.7	6.8	2.3	1.0, 1.4 (Et)
1k: (*S*)-	Et	*o*-Tol	1.8	2.2	3.9	7.2−7.4	2.5	1.0, 1.4 (Et)
1l: (*S*)-	Et	2-MeOPh	1.8	2.2	3.9	6.9−7.45	3.84	1.1, 1.45 (Et)
1m: (*S*)-	Ph	SPh	3.04 (13.7, 7.8)	2.43 (6.6)	3.85	7.05−7.6		2.74 (O*H*)
1n: (±)-	Ph	NPh_2	3.73 (15.3, 9.1)	2.36 (6.2)	4.0	6.8−7.5		

[a] R′ in PR'_2 for **1a−1l**, donor group of **1m**, **1n**.

Experimental Section

General: All manipulations involving phosphanes were carried out under argon by means of standard Schlenk techniques and were monitored by TLC (Macherey Nagel Co., Polygram SIL G/UV_{254}). All solvents were dried by standard methods[24] and distilled under argon. The solvents $CDCl_3$, CD_2Cl_2, [D_6]DMSO, and [D_8]THF used for NMR-spectroscopic measurements were degassed by three successive "freeze-pump-thaw" cycles and dried with 4-Å molecular sieves. − NMR: Bruker Avance DPX 200 at 200.12 MHz (^{1}H), 50.323 MHz (^{13}C{^{1}H}), 81.015 MHz (^{31}P{^{1}H}), T = 298 K, unless stated otherwise; chemical shifts (δ) in ppm with respect to $CHCl_3$ (^{1}H: δ = 7.27; ^{13}C: δ = 77.0) and CH_2Cl_2 (^{1}H: δ = 5.32; ^{13}C: δ = 53.5) as internal standards. ^{31}P chemical shifts (δ) in ppm with

Table 10. ^{31}P{^{1}H}- and ^{13}C{^{1}H}-NMR data of ligands **1a−1n**[a]

	R	R′[a]	PR_2 δ (^{31}P)	PR'_2 δ (^{31}P)	CH_2PR_2 δ, $^3J_{CP}$, $^1J_{CP}$	$CH_2PR'_2$ δ, $^3J_{CP}$, $^1J_{CP}$	CH−O δ, $^2J_{CP}$,$^2J_{CP}$	C_{Ar} δ	C_{Ar}−P δ, $^1J_{CP}$	C_{Ar}−Z[b] δ, $^2J_{CP}$	aryl subst. δ
1a: (*S*)-	Ph	3,5-Me_2Ph	−25.3	−26.1	38.5−39.0		68.1, 17	128.9−133.6	138.1−138.4		21.8
1b: (*R*)-	*o*-Tol	Ph	−47.1	−25.0	37.8, 7, 13	39.4, 7, 13	67.9, 17	126.7−134.1	136.6, 11 138.8, 11	141.8, 22	21.6
1c: (*S*)-	*o*-Tol	DBP	−47.3	−22.9	37.9, 7, 14	40.1, 7, 22	68.5	125.9−131.7	136.4	143.6	
1d: (*S*)-	Ph	Mes	−24.6	−33.1	39.2, 8, 14	38.6, 9, 15	68.6	128.8−133.6		138−143	21−24
1e: (*S*)-	Mes	DBP	−31.1	−20.3	38.5, 8, 15	40.4, 8, 21	69.0	121.7−143.2			21−24
1f: (*S*)-	2-MeOPh	Mes	−41.4	−29.8	36.5, 8, 14	38.8, 8, 15	68.3	111.0−134.1	125.8	138−143 161.6, 13	20.9−23.6 (Mes) 55.8 (OMe)
1g: (*S*)-	Ph	2-MeOPh	−22.4	−42.5	38.8, 8, 14	36.7, 8, 14	68.3, 17	110.9−134.1	139.3, 13	161.6	55.5
1h: (*S*)-	Ph	2-EtPh	−23.0	−48.7	38.9, 9, 13	39.4, 10, 14	68.0	126.5−133.0	136.4, 13 139.1, 13	148.9, 24	15.9, 28.0
1i: (*S*)-	Ph	2-Me_2NPh	−21.0	−41.7	40.1, 8, 16	38.7, 7, 14	67.7, 13	119.2−133.7	137.4, 139.6	157.7	45.3
1j: (*S*)-	Et	Mes	−30.0	−32.9	37.4, 7, 15	38.7, 9, 15	69.0, 15	130.3−133.0		138−143	21−23
1k: (*S*)-	Et	*o*-Tol	−27.5	−43.9	37.5−38.0		68.3	126.5−131.8	136.6	142.8	21.5, 22.0
1l: (*S*)-	Et	2-MeOPh	−25.8	−45.2	36.5, 7, 13	36.5, 8, 14	68.7, 15, 18	110.9−133.4	126.0, 15	161.8	
1m: (*S*)-	Ph	SPh	−24.0		35.8, 13	42.4, 9	67.6, 17	126.2−132.8	137.9, 135.1		
1n: (±)-	Ph	NPh_2	−24.8		34.3, 15	59.3, 9	66.9, 15	117.6−132.7	148.1		

[a] R′ in PR'_2 for **1a−1l**, donor group of **1m**, **1n**. − [b] Z = aryl substituent.

Table 11. Synthesis and analytical data of ligands **1o−1u**

	electrophile	eluent (R_f)	yield (%)	α_D^{20}	MS (*m*/*z*) [M^+][M^+ − Frag.]	$C_{calcd.}H_{calcd.}$ $C_{found}H_{found}$	MS (EI) [M^+ calcd./found]
1o:	H_3CI	−	76		442 365 [$-C_6H_5$]	76.01, 6.38 74.99, 6.57	
1p: (*R*)-	H_3CI	−	71	−	470 379 [$-C_7H_7$]	−	
1q: (*R*)-	Me_3SiCl	−	88	4.3 ± 0.8	528 437 [$-C_7H_7$]	72.70, 7.24 71.54, 7.30	
1r: (*R,S*)-	X[a]	PE/Et_2O 3:1 (0.8)	40	11.6 ± 0.5	526 435 [$-C_7H_7$]	77.54, 7.66 76.14, 7.64	526.2565 526.2560
1s: (*S*)-	Me_3SiCl	PE/Et_2O 2:1 (0.69)	44	−11.5 ± 0.6	560 483 [$-C_6H_5$]	68.55, 6.83 63.37, 7.39	560.2103 560.2084
1t: (*S,S*)-	X[a]	PE/Et_2O 4:1 (0.18)	45	−20.0 ± 0.5	559 452 [$-C_7H_7O$]	73.10, 7.22 72.25, 7.10	
1u[b]: (*S*)-	Y[c]	PE/Et_2O 2:1 (0.46)	53	−	665 546 [$-C_9H_{11}$]	−	

[a] X = $H_3CCH_2CH(CH_3)CH_2OSO_2C_6H_4CH_3$. − [b] See Experimental Section. − [c] Y = $H_2C{=}CH(CH_2)_9OSO_2C_6H_4CH_3$.

Table 12. ^{1}H-NMR data of ligands **1o−1u**

	R	R′	R″	CH_2P δ	CH−O δ	H_{Ar} δ	aryl subst. δ	(R″)H δ
1o:	Ph	Ph	CH_3	2.74−2.9	3.59	7.48−7.71		3.34
1p: (*R*)-	*o*-Tol	Ph	CH_3	2.2−2.4	3.36	7.14−7.41	2.5	3.15
1q: (*R*)-	*o*-Tol	Ph	$SiMe_3$	2.55−2.85	4.14	7.2−7.7	2.55	0.02
1r: (*R,S*)-	*o*-Tol	Ph	X[a]	2.5−2.7	3.6	7.25−7.58	2.51, 2.59	0.9−1.5, 3.2
1s: (*S*)-	Ph	2-MeOPh	$SiMe_3$	2.5−2.85	4.19	7.0−7.6	3.85	0.05
1t: (*S,S*)-	Ph	2-MeOPh	X[a]	2.54−2.73	3.6	6.9−7.6	3.83	0.9−1.5, 3.3
1u: (*S*)-	Ph	Mes	Y[b]	3.0−3.4	3.5	7.2−7.4	2.28	1.36, 5.0, 5.81

[a] X = (*S*)-$H_3CCH_2CH(CH_3)CH_2$. − [b] Y = $H_2C{=}CH[CH_2]_9$.

respect to 85% H_3PO_4 (^{31}P: δ = 0) as external standard. – MS (EI): Finnigan MAT 8320: Fast-atom bombardment (FAB) xenon, matrix: 4-nitrobenzyl alcohol. – HR-MS(EI): Jeol JMS-700. – Melting points: Gallenkamp MFB-595010; uncorrected values. – Optical rotations: Jasco DIP310, 10-cm cell, Na-D line (λ = 589 nm). – GC/MS: HP 5890II (GC) interfaced to an HP5981 (MS) (Hewlett Packard). – Elemental analyses: Microanalytical Laboratory of the Organisch-Chemisches Institut, Universität Heidelberg.

Table 13. $^{31}P\{^1H\}$- and $^{13}C\{^1H\}$-NMR data of ligands **1o–1u**

	R	R′	R″	PR_2 δ (^{31}P)	PR'_2 δ (^{31}P)	CH_2PR_2 δ, $^3J_{CP}$, $^1J_{CP}$	$CH_2PR'_2$ δ, $^3J_{CP}$, $^1J_{CP}$	CH–O δ, $^2J_{CP}$, $^2J_{CP}$	C_{Ar} δ	C_{Ar}–P δ, $^1J_{CP}$	C_{Ar}–Z[d] δ, $^2J_{CP}$	aryl subst. δ	R″ δ
1o:	Ph	Ph	CH_3	–23.6		33.8, 8, 15	77.6	128.9–133.8	139.8			56.9	
1p: (*R*)-	*o*-Tol	Ph	CH_3	–46.3	–23.9	34.5, 8, 15	35.8, 8, 15	77.3	126.3–133.6	137.3, 139.1, 13	142.7	21.4, 21.9	56.7
1q: (*R*)-	*o*-Tol	Ph	$SiMe_3$	–44.6	–21.6	37.9, 8, 15	39.3, 9, 14	69.5, 18	126.4–133.5	137.6, 14 149.8	142.7, 26	21.5	0.4
1r: (*R,S*)-	*o*-Tol	Ph	X[a]	–44.6	–21.7	34.8, 9, 15	36.7, 8, 15	76.3	126.4–133.6	137.6, 13 139.8, 13	142.6, 26	21.3	11.7, 16.9, 26.6, 35.7, 74.6
1s: (*S*)-	Ph	2-MeOPh	$SiMe_3$	–39.1	–21.3	38.9, 9, 14	36.2, 9, 15	70.2, 17, 22	110.9–134.1	140.1	161.8, 13	55.9	0.05
1t: (*S,S*)-	Ph	2-MeOPh	X[a]	–38.2	–21.4	36.2, 9, 14	32.7, 8, 15	76.9	110.9–134.0	126.2, 12 139.9, 14	161.7, 13	55.8	11.7, 16.9, 26.6, 35.7, 74.5
1u[b]: (*S*)-	Ph	Mes	Y[c]	–22.8	–30.6								

[a] X = (*S*)-$H_3CCH_2CH(CH_3)CH_2$. – [b] See Experimental Section. – [c] Y = $H_2C{=}CH[CH_2]_9$. – [d] Z = aryl substituent.

Table 14. ^1H-NMR data of complexes **2**[a,b]

	CH_2 δ	CH–O δ	CH_{COD} δ	H_{Ar} δ	CH_3/other δ
2a: (*S*)-	2.1–3.1	3.78	4.37, 5.0	6.9–7.7	2.32, 2.35
2b: (*R*)-	2.1–3.0	3.9	4.2–4.9	7.3–7.7	2.38, 2.41
2c: (*S*)-	2.0–3.2	3.9	4.0–4.7	7.0–8.1	2.17, 2.20
2d: (*S*)-	2.1–2.6 3.1 [1 H] CH_2PMes_2	3.6	3.97, 4.37, 4.47, 4.79	6.8–7.3 (Mes) 7.1–8.2 (Ph)	1.76, 2.05, 2.31, 2.41, 2.71, 3.56
2e: (*S*)-	1.9–2.6, 3.38 [1 H] CH_2PMes_2	3.8	4.23, 4.74	6.8–7.3 (Mes) 7.6–8.1 (DBP)	1.78, 2.20, 2.37, 2.41, 3.0, 3.72
2f: (*R*)-	2.1–2.9 2.93 [1 H] CH_2PMes_2	4.15	4.1–4.4	6.6–7.5, 7.78 + 9.22 (Mes)	1.70, 2.05, 2.32, 2.43, 2.62, 3.66, 3.73, 4.01 (OCH_3)
2g: (*S*)-	2.1–2.5, 2.55, 3.0 [1 H] $CH_2PR'_2$	3.71	4.25–4.6	7.1–7.8	3.86, 3.93
2h: (*S*)-	2.1–3.0		3.9–4.9	7.3–8.2	1.1–1.5, H_3CCH_2
2j: (*S*)-	1.7–2.8	3.69	4.0, 4.6	6.8–7.1	1.68, 2.2–2.4, 2.83, 1.2–1.4 (Et)
2k: (*S*)-	1.0–3.0	3.5	4.72, 5.2	6.8–7.8	1.2–1.4 (Et)
2l: (*S*)-	2.0–2.8		4.1–4.4	7.0–7.7	3.9, 1.1–1.7 (Et)
2m: (*S*)-	2.91–3.35, 2.0–2.5 (COD)	4.25	4.25	7.44–8.0	
2o:	2.25–2.8	3.33	4.43, 4.97	7.4–7.8	3.23 (H_3CO)
2p: (*R*)-	2.1–3.0	3.45	4.1–4.9	7.4–7.8	3.11 (H_3CO)
2q: (*R*)-	1.8–3.0		3.9–4.9	7.0–8.1	–0.1 $(H_3C)_3Si$
2r: (*R,S*)-	2.0–3.1		3.9–5.0	7.0–8.4	0.8 (H_3C) 0.96 (CH), 1.22 (CH_2)
2s: (*S*)-	2.3–2.8		4.45	7.16–7.6	–0.1 (H_3CSi) 3.9 (OCH_3)
2t: (*S,S*)-	2.1–2.8	3.55	4.3–4.7	7.1–7.9	0.8 (H_3C), 0.96 (CH), 1.29 (CH_2)
2u: (*S*)-	2.1–2.8		4.01, 4.38, 4.51, 4.82	6.9–8.2	0.9–1.5 (CH_2), 1.7, 2.1–2.8, 3.4–3.7 (Mes) 5.0 (H_2C), 5.9 (CH)
2v:	2.1–2.6, 2.85	3.80	4.41, 4.96	7.2–7.8	–
2w: (*R*)-	2.8–2.85	3.80	4.40, 4.98	7.24–7.75	2.40

[a] Due to dynamic phenomena (see text) most of the signals are rather broad. Depending on the appearance of the spectra, either ranges are given in the table, or, if predominant peaks are observed in the corresponding ranges, the shifts of these peaks are given. – [b] For complexes **2i**, **2n** see Experimental Section.

− Catalytic hydrogenations were performed in a hydrogenation apparatus according to Marhan (Normag) (1 bar) or in an HR 250 stainless steel high-pressure laboratory reactor (Berghof/Maasen GmbH) (30 bar). Yields were determined by ^{1}H-NMR analysis; the *ee* values were determined by GC/MS (column: Chirasil L-Val, Chrompack GmbH).

Materials: Silica gel (Kieselgel z.A. 0.06−0.2 mm, J. T. Baker Chemicals B.V.) used for chromatography was degassed at 1 mbar for 24 h and saturated with argon. A solution of 2.5 M *n*BuLi in hexanes was used for deprotonations. (*S*)- and (*R*)-epichlorohydrin (A) (Aldrich, 97% *ee*) were degassed (see above) and checked for optical purity by measurement of their specific rotations ($|[\alpha]_D^{20}|$ = 34.3[25]). $HPEt_2$,[26] $HPPh_2$,[27] HP(*p*-Tol)$_2$,[27] HP(*o*-Tol)$_2$,[28] HP(*m*-Xyl)$_2$,[29] $HPMes_2$,[30] HP(2-EtPh)$_2$,[31] HP(2-MeOPh)$_2$,[32] HP(2-Me_2NPh)$_2$,[32,33] DBPH,[34] and [Rh(COD)Cl]$_2$[35] were prepared according to or by adaptation of literature procedures. All other chemicals were obtained from commercial suppliers and used without further purification.

Ligand Synthesis

General Procedure for the Synthesis of Ligands 1a−1n: 5−12 mmol of phosphane R_2PH for the generation of nucleophile I (Table 8) was dissolved in 30 mL of THF and deprotonated by the dropwise addition of *n*BuLi at −70°C. This solution was stirred for 10 min. Meanwhile, 5−12 mmol of epichlorohydrin was dissolved in 20 mL of THF and the solution was cooled to −70°C. At this temperature, the previously prepared phosphide solution was added in a dropwise manner over a period of 30 min. After warming to room

Table 15. $^{13}C\{^1H\}$-NMR data of complexes **2**[a]

	CH_2 ($^1J_{CP}$, $^3J_{CP}$)	CH−O δ	CH_{COD} δ	C_{Ar}[b] δ	CH_3/other δ
2a: (*S*)-	30.8 (COD) 34.6 (8,12) 35.1 (8,12)	64.4	98.3, 99.1, 103.7, 104.5	129.0−134.3, 139.3 (C_q)	21.5
2b: (*R*)-	27.0−33.0	65.3	99.0−104.0	126.5−133.5, 143.0 (C_q)	23.1, 23.8
2c: (*S*)-	30.3, 33.2	66.0	101.3, 106.3	122.4−135.8, 142.8 (C_q)	23.9
2d: (*S*)-	30.1−35.4	65.7	92.3, 94.8, 99.4, 106.7	129.5−136.2, 124.3 [C_i(Mes)], 141.4−144.3 (C_q)	20.8−27.1
2e: (*S*)-	28−28.6 (COD), 32.0, 38.2	65.4	95.6, 96.9, 98.4, 108.5	122.0−132.0 140.0−145.0 (C_q)	20.9, 21.0, 22.5, 24.7, 26.4, 27.7
2f: (*R*)-	28.1−33.3	66.2	89.7, 94.9, 98.6, 104.6	112.3−144.3 117.2 (C_r-Anisyl) 160.1−162.3 (C_q)	20.8−26.9, 56.0 (OCH_3)
2g: (*S*)-	30.3−32.7	65.4	97.9−102.7	112.3−121.4 (Anisyl) 129.6−136.0 160.9 (C_q−OCH_3)	56.1
2h: (*S*)-	28−29.5 (COD) 31.0−33.0	65.2	98.0−104.5	126.4−134.5 149.3 (C_q−Et)	14.4, 32.0
2j: (*S*)-	18.6−35.3	69.0	93.5, 106.3	130.0−142.0	
2k: (*S*)-	28.8−33.0	64.7	97.1, 99.2, 103.3	126.2−133.3 140.7−143.1 (C_q)	8.4, 21.0 (Et) 23.2, 23.9
2l: (*S*)-	29.9−32.6	66.2	96.2, 97.0 112.2, 116.7	121.1 ($C_{Ar}C_qOCH_3$), 131−134.7, 160.8 (C_q)	8.6, 19.5 (Et) 56.0
2m: (*S*)-	30.0−31 (COD) 35.1 (23) 44.5 (CH_2S)	65.8		129.2−135.3	
2o:	30.6, 31.5	73.2	99.8, 104.2	129.1−134.2	56.0 (OCH_3)
2p: (*R*)-	27.0−33.5	74.5	98.0−104.0	126.5−133.3 141.7 (C_q)	23.1−23.7 56.2 (H_3CO)
2q: (*R*)-	27.0−33.5	65.9	97.0−104.5	126.5−133.3 140.3 (C_q)	−0.1 (C−Si) 23.3
2r: (*R,S*)-	27.0−33.3	72.9	99.0−104.5	126.6−134.2 141.3 (C_q)	11.4, 16.6, 26.3, 35.3, 74.0 (R′′) 23.1 (Tol)
2s: (*S*)-	30.1−33.6	66.0	99.5, 102.5	112.2 ($C_{Ar}C_qOCH_3$), 121.4−134.1 160.8 (C_q)	−0.2 (C−Si), 56.1 (OCH_3)
2t: (*S,S*)-	27.0−31.0	73.1	98.0−103.0	121.2−134.5 160.9 (C_q)	11.4, 16.6, 26.3, 35.2, 73.9 (R′′) 56.0 (OCH_3)
2u: (*S*)-	20.8−34.2	68.7	92.4, 94.9, 97.8, 107.0	129.4−139.6	72.9 (H_2C), 114.3 (CH) (R′′)
2v:	30.6 (COD), 34.6	64.2	99.1, 104.2	129.4−134.1	−
2w: (*R*)-	30.6 (COD), 34.6	65.3	98.8, 103.9	125.7−134.5 143.0 (C_q)	21.5

[a] For complexes **2i**, **2n** see Experimental Section. − [b] C_q = C_{Ar}−C, C_i = C_{Ar}−P.

temperature, the orange solution was stirred for 30−120 min (Table 8) and then cooled to −70°C once more. Then, a solution of 1 equiv. of nucleophile II (phosphane, thiol, or amine), generated by a deprotonation procedure analogous to that described for nucleophile I, was added in a dropwise manner to the cooled reaction mixture over a period of 30 min. The resulting mixture was stirred at room temperature for 2−16 h (Table 8). The solvent was then evaporated in vacuo (10^{-1} mbar) and the residue was suspended in 30 mL of diethyl ether. 20 mL of acetate buffer was added, the organic phase was separated, and the aqueous layer was extracted with three 20-mL portions of diethyl ether. The combined organic phases were dried with Na_2SO_4, the solvent was evaporated in va-

Table 16. Crystal data[a]

Compound	**2v**[b]	**2o**·CH_2Cl_2	**2b**[c]·CH_2Cl_2·1/2Et_2O	**2d**·Et_2O
Formula	$C_{35}H_{38}F_6OP_3Rh$	$C_{36}H_{40}F_6OP_3Rh$	$C_{37}H_{42}F_6OP_3Rh$	$C_{41}H_{50}F_6OP_3Rh$
Molecular mass	784.470	798.530	812.550	868.660
Crystal system	orthorhombic	monoclinic	triclinic	triclinic
Space group	$Pna2_1$	$C2/c$	$P1$	$P1$
Lattice constants	a = 1852.9(3)	a = 3129.9(5)	a = 1042.1 (1)	a = 1205.8(2)
	b = 1131.9(2)	b = 1280.9(1)	b = 1243.0 (2)	b = 1267.4(2)
	c = 1628.3(3) pm	c = 1901.9(1) pm	c = 1708.7 (2) pm	c = 1706.3(3) pm
	α = 90	α = 90	α = 79.27 (1)	α = 87.23(1)
	β = 90	β = 88.56(1)	β = 77.38 (1)	β = 70.44(1)
	γ = 90°	γ = 90°	γ = 67.31 (1)°	γ = 63.05(1)°
Cell volume	3415 × 10^6 pm^3	7623 × 10^{-6} pm^3	1980 × 10^6 pm^3	2174 × 10^6 pm^3
Molecular units per cell	Z = 4	Z = 8	Z = 2	Z = 2
Density (calculated)	1.526 g/cm^3	1.536 g/cm^3	1.453 g/cm^3	1.439 g/cm^3
Temperature	200 K	200 K	200 K	200 K
Number of reflections for cell refinement	30	32	34	25
Scan range	4.2° < 2Θ < 56.0°	3.4° < 2Θ < 50.0°	4.1° < 2Θ < 54.0°	3.6° < 2Θ < 48.0°
Method	ω scan, Δω = 0.47°	ω scan, Δω = 0.60°	ω scan, Δω = 0.60°	ω scan, Δω = 0.50°
scan speed [° min^{-1}]	8.0	15.0	10.0	12.0
Number of measured reflections	4263	6641	9131	11043
unique reflections	4263	6511	9131	10613
observed reflections ($I \geq 2\sigma$)	3070	4437	8324	10044
Number of parameters refined	382	489	898	1019
Maximum of residual Electron density	1.23 × 10^{-6} e/pm^3	0.51 × 10^6 e/pm^3	1.26 × 10^{-6} e/pm^3	0.59 × 10^{-6} e/pm^3
Agreement factors (F^2 refinement)	R_1 = 0.087	R_1 = 0.052	R_1 = 0.047	R_1 = 0.032
	R_w = 0.286	R_w = 0.132	R_w = 0.132	R_w = 0.094

Compound	**2g**[c]	**2f**[d]·CH_2Cl_2	**2e**[d]·CH_2Cl_2	**2c**·Et_2O
Formula	$C_{37}H_{42}F_6O_3P_3Rh$	$C_{43}H_{54}F_6O_3P_3Rh$	$C_{41}H_{48}F_6OP_3Rh$	$C_{37}H_{40}F_6OP_3Rh$
Molecular mass	844.530	928.70	866.650	810.540
Crystal system	monoclinic	monoclinic	orthorhombic	monoclinic
Space group	$P2_1$	$P2_1$	$P2_12_12_1$ #19	$P2_1$
Lattice constants	a = 1485.0(3)	a = 1516.5(4)	a = 1072.9(2)	a = 982.4(1)
	b = 1311.3(2)	b = 1522.9(3)	b = 1433.8(2)	b = 1630.5(2)
	c = 2041.2(4) pm	c = 2050.4(5) pm	c = 2695.3(3) pm	c = 1275.2(1) pm
	α = 90	α = 90.	α = 90	α = 90
	β = 108.72(1)	β = 110.49(2)	β = 90	β = 71.60(1)
	γ = 90°	γ = 90°	γ = 90°	γ = 90°
Cell volume	3764 × 10^6 pm^3	4435 × 10^6 pm^3	4146 × 10^6 pm^3	1938 × 10^6 pm^3
Molecular units per cell	Z = 4	Z = 4	Z = 4	Z = 2
Density (calculated)	1.490 g/cm^3	1.452 g/cm^3	1.524 g/cm^3	1.512 g/cm^3
Temperature	298 K	200 K	200 K	200 K
Number of reflections for cell refinement	31	31	30	29
Scan range	2.1° < 2Θ < 47.0°	2.1° < 2Θ < 50.2°	3.0° < 2Θ < 51.0°	4.2° < 2Θ < 50.1°
Method	ωscan, Δω = 0.43°	ωscan, Δω = 0.50°	ωscan, Δω = 0.54°	ωscan, Δω = 0.45°
scan speed [° min^{-1}]	12.0	8.0	8.0	10.0
Number of measured reflections	12137	7629	8612	7538
unique reflections	11117	7386	7565	6634
observed reflections ($I \geq 2\sigma$)	8730	6477	7189	6427
Number of parameters refined	853	1063	572	496
Maximum of residual electron density	0.59 × 10^{-6} e/pm^3	2.23 × 10^{-6} e/pm^3	0.45 × 10^{-6} e/pm^3	0.46 × 10^{-6} e/pm^3
Agreement factors (F^2 refinement)	R_1 = 0.045	R_1 = 0.067	R_1 = 0.027	R_1 = 0.030
	R_w = 0.113	R_w = 0.218	R_w = 0.062	R_w = 0.087

[a] The crystals of **2** tend to contain solvate molecules. The number and type of solvate molecules found per formula unit is given in the column header. − [b] Disorder of the COD ligand and of two of the aryl groups greatly reduces the accuracy of the structure determination. − [c] Disorder of the two PF_6 counterions. − [d] Disorder of one PF_6 counterion.

cuo, and the oily white residue was purified by column chromatography (silica gel, eluent and R_f as given in Table 8). Analytical difficulties arose in part due to the hygroscopic nature and the sensitivity to oxidation of the ligands when analytical samples were prepared without inert gas protection.

General Procedure for the Etherification of Ligands 1a−1n: 1 mmol of ligand was dissolved in 50 mL of freshly dried THF and the resulting solution was cooled to −5°C. At this temperature, 2 equiv. of KO*t*Bu were added and the solution was stirred for 2 min.

Methylation: 2 equiv. of methyl iodide were added to the above solution and the progress of the reaction was monitored by TLC. After completion of the reaction (maximum reaction time 30 min), the solvent and excess methyl iodide were evaporated in vacuo. The residue was dissolved in 30 mL of diethyl ether and the solution was filtered to remove potassium chloride. Removal of the solvent yielded the methylated ligands in an analytically pure state (Table 11).

Silylation: 1.6 equiv. of Me_3SiCl were added to the above solution and the progress of the reaction was monitored by TLC. After completion of the reaction (maximum reaction time 30 min), the solvent and excess Me_3SiCl were evaporated in vacuo. The residue was dissolved in 30 mL of CH_2Cl_2 and the solution was filtered to remove potassium chloride. If, after removal of the solvent, the products were not found to be analytically pure, they were further purified by column chromatography (Table 11).

Alkylation: 1.5 equiv. of alkyl tosylate were added to the reaction mixture and the ensuing reaction was monitored by TLC. The solution was stirred for 30 min, allowed to warm to room temperature, and then stirred for 6 h. If the conversion was not complete, the reaction mixture was cooled to −5°C once more, 0.5 equiv. of KO*t*Bu and alkyl tosylate were added and, after warming to room temperature, the solution was stirred for a further 4 h. The solvent was then evaporated in vacuo and the residue was purified by column chromatography (silica gel, eluent and R_f as given in Table 11). Compound **1u** could not be obtained in an analytically pure state because of identical R_f values for both the product and the corresponding long-chain alcohol. Therefore, the crude product **1u** was used to synthesize **2u**, which could be purified by column chromatography.

General Procedure for the Synthesis of Complexes 2: 0.5 equiv. of di-μ-chlorobis(η^4-1,5-cyclooctadiene)dirhodium(I) ($[Rh(COD)Cl]_2$) was dissolved in 10 mL of CH_2Cl_2 and a solution of 1.2 equiv. of potassium hexafluorophosphate in 5 mL of THF/acetone (1:1) was added. The mixture was stirred for 2 min. 1 mmol (1 equiv.) of the appropriate ligand was dissolved in 30 mL of CH_2Cl_2 and the resulting solution was added to the above mixture in a dropwise manner. After stirring for 30 min, the solvent was evaporated in vacuo, the residue was redissolved in 5 mL of CH_2Cl_2, and the solution was filtered through Na_2SO_4. Complexes **2** were precipitated as orange powders upon addition of 20 mL of diethyl ether. Further purification was generally not necessary but could be achieved by washing with diethyl ether, by recrystallization, or by chromatography. Chromatography on silica gel was possible when CH_2Cl_2 solutions of **2** were applied to a column with CH_2Cl_2 as the mobile phase. Elution with CH_2Cl_2 removed contaminants while compounds **2** did not noticeably migrate under these conditions. They were subsequently eluted with CH_2Cl_2/Et_2O or THF/Et_2O mixtures. On evaporation of the solvent from the eluate, the purified compounds **2** were obtained in microcrystalline form. The syntheses of the complexes containing an amine donor function (**2i**, **2n**), even under varied reaction conditions, invariably resulted in a mixture of different coordination products, as was clearly evident from the ^{31}P-NMR spectra. In none of these cases could a single product be separated by recrystallization or column chromatography.

X-ray Structure Determinations:[36] Single crystals were obtained by the layering technique. Exploratory experiments with various solvents (CH_2Cl_2, THF, Et_2O) and mixtures thereof had to be performed in order to obtain crystals of sufficient quality. Suitable crystals were taken directly from the mother liquor, immersed in perfluorinated polyether oil, and fixed to a glass rod at 200 K. In the case of **2g**, for which the data were collected at 298 K, the crystal was fixed in a Lindemann capillary. The measurements were made with a Siemens P4 four-circle diffractometer (equipped with a low-temperature device) using graphite-monochromated Mo-K_α radiation. All calculations were performed using the SHELXTPLUS[37] software package. Structures were solved by direct methods with the SHELXS-86 program[37a] and refined with the SHELX-93 program.[37b] Graphical handling of the structural data during solution and refinement was performed with XPMA.[38] Absorption corrections (ψ scan, $\Delta\psi = 10°$) were applied to the data. Atomic coordinates and anisotropic parameters of the non-hydrogen atoms were refined by full-matrix least-squares calculations. Data pertaining to the structure determinations are compiled in Table 16.

Acknowledgments

We are indebted to the Deutsche Forschungsgemeinschaft and the Fonds der Chemischen Industrie for financial support. A generous loan of rhodium(III) chloride by the DEGUSSA AG is gratefully acknowledged. We wish to thank T. Jannack for mass-spectrometric analysis and Dr. J. Groß for his help with high-resolution mass spectra. The continued enthusiasm and patience of Dr. Laszlo Zsolnai in solving crystal structures over more than two decades has helped a lot. Dr. Zsolnai died April 26, 1998.

[1] V. Caplar, G. Comisso, V. Sunjic, *Synthesis* **1981**, 85−116.
[2] M. Nógradi, *Stereoselective Synthesis*, VCH, Weinheim, **1995**.
[3] [3a] J. Halpern, D. P. Riley, A. S. Chan, J. J. Pluth, *J. Am. Chem. Soc.* **1977**, *99*, 8055−8057. − [3b] A. S. Chan, J. Halpern, *J. Am. Chem. Soc.* **1980**, *102*, 838−840. − [3c] P. S. Chua, N. K. Roberts, B. Bosnich, S. J. Okrasinski, J. Halpern, *J. Chem. Soc., Chem. Commun.* **1981**, 1278−1280. − [3d] J. M. Brown, P. A. Chaloner, *Tetrahedron Lett.* **1978**, *21*, 1877−1880. − [3e] C. R. Landis, J. Halpern, *J. Am. Chem. Soc.* **1987**, *109*, 1746−1754.
[4] H. B. Kagan, T. B. Dang, *J. Chem. Soc., Chem. Commun.* **1971**, 481−483.
[5] H. B. Kagan, T. B. Dang, *J. Am. Chem. Soc.* **1972**, *94*, 6429−6433.
[6] H. Brunner, *Handbook of Enantioselective Catalysis with Transition Metal Compounds*, VCH, Weinheim, **1993**.
[7] J. M. Brown, P. A. Chaloner, B. A. Murrer, D. Parker, *A. C. S. Symp. Ser.* **1980**, *119*, 169−194.
[8] P. McNeil, N. K. Roberts, B. Bosnich, *J. Am. Chem. Soc.* **1981**, *103*, 2273−2280.
[9] J. Bakos, I. Tóth, B. Heil, G. Szalontai, L. Párkányi, V. Fülöp, *J. Organomet. Chem.* **1989**, *370*, 263−276.
[10] [10a] S. R. Niketic, F. Woldbye, *Acta. Chem. Scand.* **1973**, *27*, 621−642. − [10b] M. Kojima, M. Fufita, J. Fujita, *Bull. Chem. Soc. Jpn.* **1977**, *50*, 898−906.
[11] See however modelling of tripod metal templates: S. Beyreuther, J. Hunger, G. Huttner, S. Mann, L. Zsolnai, *Chem. Ber.* **1996**, *129*, 745−757.
[12] J. Hunger, S. Beyreuther, G. Huttner, K. Allinger, U. Radelof, L. Zsolnai, *Eur. J. Inorg. Chem.* **1998**, *6*, 693−702.
[13] J. Scherer, G. Huttner, M. Büchner, *Chem. Ber.* **1996**, *129*, 697−713.
[14] J. Scherer, G. Huttner, M. Büchner, J. Bakos, *J. Organomet. Chem.* **1996**, *520*, 45−58.
[15] E. G. Thaler, K. G. Caulton, *Organometallics* **1990**, *9*, 1871−1876.

[16] E. G. Thaler, K. Folting, K. G. Caulton, *J. Am. Chem. Soc.* **1990**, *112*, 2664−2672.
[17] W. O. Siegl, S. J. Lapporte, J. P. Collmann, *Inorg. Chem.* **1971**, *10*, 2158−2165.
[18] H. Brunner, A. Sicheneder, *Angew. Chem.* **1988**, *100*, 730−731, *Angew. Chem. Int. Ed. Engl.* **1988**, *27*, 718−719.
[19] [19a] Th. Seitz, A. Muth, G. Huttner, Th. Klein, O. Walter, M. Fritz, L. Zsolnai, *J. Organomet. Chem.* **1994**, *469*, 155−162. − [19b] Th. Seitz, G. Huttner, M. Büchner, *Z. Naturforsch. B* **1994**, *49*, 1813−1817.
[20] P. Schober, R. Soltek, G. Huttner, L. Zsolnai, K. Heinze, *Eur. J. Inorg. Chem.* **1998**, 1407−1415.
[21] [21a] A. Frick, Diplomarbeit, Universität Heidelberg, **1996**. − [21b] Publication in preparation.
[22] A. Jacobi, G. Huttner, U. Winterhalter, *J. Organomet. Chem.*, in press. It thus appears that with six-membered chelate cycles, hydroxy or alkoxy functionalization at the chelate backbone does not drastically influence reactivity. This is in contrast to the observations made for larger, more flexible chelate cycles, where this type of substitution interferes with reactivity as well as selectivity. For a review see: J. Holz, M. Quirmbach, A. Börner, *Synthesis* **1997**, 983−1006.
[23] [23a] W. S. Knowles, B. D. Vineyard, M. J. Sabacky, *J. Chem. Soc., Chem. Commun*. **1972**, 10−11. − [23b] B. D. Vineyard, W. S. Knowles, M. J. Sabacky, D. J. Weinkauff, *J. Am .Chem. Soc.* **1975**, *97*, 2567−2568. − [23c] B. D. Vineyard, W. S. Knowles, M. J. Sabacky, G. L. Bachmann, *J. Am. Chem. Soc.* **1977**, *99*, 5946−5952.
[24] *Organikum*, Deutscher Verlag der Wissenschaften, Berlin, **1990**.
[25] J. Baldwin, A. Raab, K. Mensler, B. Arison, D. McClure, *J. Org. Chem.* **1978**, *43*, 4876−4878.
[26] K. Issleib, A. Tzack, *Chem. Ber.* **1959**, *92*, 704−711.
[27] K. Issleib, H. O. Fröhlich, *Z. Naturforsch. B* **1959**, *14*, 349−350.
[28] [28a] F. G. Mann, E. J. Chaplin, *J. Chem. Soc.* **1937**, 527−535. − [28b] G. P. Schiemenz, *Angew. Chem.* **1968**, *80*, 559−560; *Angew. Chem. Int. Ed. Engl.* **1968**, *7*, 544−545. − [28c] C. A. Tolman, *J. Am. Chem. Soc.* **1970**, *92*, 2956−2965.
[29] M. Culcasi, Y. Berchadsky, G. Groncho, P. Tordo, *J. Org. Chem.* **1991**, *56*, 3537−3542.
[30] J. B. Lambert, J. H. So, *J. Org. Chem.* **1991**, *56*, 5960−5962.
[31] [31a] G. Schiemenz, H. Kack, *Liebigs Ann. Chem.* **1973**, 1494−1504. − [31b] C. Ziegler, R. Heck, *J. Org. Chem.* **1978**, *43*, 2941−2946.
[32] P. Budzelaar, J. Doorn, N. Meijboom, *Recl. Trav. Chim. Pays-Bas* **1991**, *110*, 420−432.
[33] L. Horner, G. Simons, *Phosphorus Sulfur* **1983**, *15*, 165−175.
[34] [34a] J. Cornforth, R. H. Cornforth, R. T. Grey, *J. Chem. Soc., Perkin Trans. 1* **1982**, 2289−2297. − [34b] E. H. Braye, I. Chaplier, R. Saussez, *Tetrahedron* **1971**, *21*, 5523−5537.
[35] G. Giordano, R. H. Crabtree, *Inorg. Synth.* **1990**, *28*, 88−90.
[36] Tables of the fractional atomic cordinates are available from the author on request. Further details of the crystal structure investigations may be obatined from the Fachinformationszentrum Karlsruhe, D-76344 Eggenstein-Leopoldshafen on quoting the depository numbers CSD-410021 (**2o**), -410022 (**2c**), -410023 (**2f**), -410024 (**2g**), -410025 (**2e**), -410026 (**2v**), -410027 (**2d**), and -410028 (**2b**).
[37] [37a] G. M. Sheldrick, *SHELX(S)-86*, University of Göttingen, **1986**. − [37b] G. M. Sheldrick, *SHELXL-93*, University of Göttingen, **1993**. − [37c] *International Tables for X-ray Crystallography*, vol. 4, Kynoch Press, Birmingham, U.K., **1974**.
[38] L. Zsolnai, G. Huttner, *XPMA*, University of Heidelberg, **1994**.

Received August 19, 1998
[I98285]